Analysis of the Dynamic Effects of An

Elastic Belt in A General Mechanical System

Yeongching Lin, Ph. D.
Mechanical Dynamics

Todd DePauw
Mechanical Dynamics

Yaqun Jiang, Ph. D.
Mechanical Dynamics

12th European ADAMS User's Conference
Sorat Hotel, Marburg, Germany
November 18, 1997

ABSTRACT

Traditional analysis of mechanical systems has been concerned with the macroscopic behavior or rigid bodies. Finite element analysis has provided the ability to construct reasonable approximations of flexible bodies. Coupling these technologies would provide acceptably accurate representations of real-world applications. However, the time required to construct and calculate the large set of non-linear equations make them too costly.

This paper presents a method, which combines the flexible body approach and the mechanical system simulation into and acceptably fast and accurate solution. The flexible belt plays an integral role in many important mechanical systems. The method consists of discretizing the belt into finite lumped masses and connecting them using force equations representing the elastic components of the belt. A typical engine accessory belt drive is provided as an example of the application of this method.

INTRODUCTION

The purpose of this paper is to discuss a model of belt driven system using ADAMS. The completed model will be used to analyze several different characteristics concerning engine accessory belt systems. The nonlinear model is used to simulate the longitudinal and transverse response of the belt driven system, as well as the belt impact dynamics and slippage of the pulleys.

Multi-body flexible dynamics method was used to determine the safety factor under design load for the mechanical and hydraulic tensioners and plastic pulley assemblies. ADAMS was used to model the geometry, and calculate static and dynamic responses. Flexible elements were used in ADAMS to solve for the static loads and dynamic loads as well as evaluate the tensioner performance. The static loads, dynamic loads, and fatigue safety factors were calculated and verified to meet the design specifications.

A preliminary part of the development cycle is to determine the safety factors for anticipated operating conditions. The engineers utilize ADAMS simulation results to predict loads and evaluate design concepts before proceeding to the final design specifications. The initial concept design is analyzed via an ADAMS analysis of the automatic tensioners subjected to static and dynamic loads that can be expected from a front-end accessory belt drive system. The primary function of the accessory belt driven system is power transmission from the crankshaft pulley to the accessory components. Accessory components include the alternator, power-steering pump, air conditioner, and the water pump.

The automatic tensioner provides a constant static tension to the accessory belt system and dynamically reacts to changes in system torque caused by the crankshaft torsional vibration during engine operation. A tensioner must also react to load variations in the accessory components. A primary function of the tensioner can be modeled as an energy dissipater to the belt driven system. Hence, the tensioner's stiffness and damping characteristics are critical to the performance of the accessory driven system. Because the design objectives require quieter and more durable engine systems and related components, the performance of the belt tensioner is critical.

This project establishes the foundation for a load analysis capability for a belt drive system, with the objective of improving product designs and quality. The successful conclusion of this project will provide automotive manufacturers and supplier personnel with the ability to better understand accessory belt designs, to more quickly determine an optimal design, and to reduce time and cost in the design process.

Approach

A flexible body in ADAMS is a collection of particles, undergoing small, linear deformations relative to a local body reference frame, *B*, while this reference frame undergoes large nonlinear global displacements and rotations. These particles are frequently the nodes of a finite element model. Since it is impractical to track the motion of the individual particles, the linear local motion is approximated as a linear combination of shape vectors or mode shapes:

The motion of the i^{th} particle is

$$r_i = \mathbf{x} + \mathbf{A}(s_i + \Phi \mathbf{q})$$

Where

- **X** defines the position vector from the global origin to the local reference frame, *B*.
- **A** is the direction cosines of the orientation between the global origin to *B*.
- r_i is the undeformed location of the i^{th} particle in *B*.
- **Φ** defines the contribution of the mode shapes to the i^{th} particle.
- **q** is the vector of modal amplitudes.

Using Euler angels to represent orientation, the generalized coordinates of motion are

$$\xi = \begin{Bmatrix} x \\ y \\ z \\ \psi \\ \theta \\ \phi \\ q_j, j = 1, m \end{Bmatrix} = \begin{Bmatrix} \mathbf{x} \\ \mathbf{\Psi} \\ \mathbf{q} \end{Bmatrix}$$

Where

x, y, and z are the locations of B relative to the global origin.
ψ, θ, and ϕ are the euler angles of B relative to the global origin.
q_j are the modal amplitudes of the m contributing mode shapes.

The velocity of the i^{th} particle can be shown to be:

$$v_i = \left[I - A\left(\tilde{s}_i + \tilde{\Phi}_i q\right) B A \Phi_i \right] \dot{\xi}$$

From which we obtain an expression for the kinetic energy:

$$T = \frac{1}{2} \sum_{i=1}^{N} m_i v_i^T v_i = \frac{1}{2} \dot{\xi}^T M(\xi) \dot{\xi}$$

After deriving the much simpler expressions for the potential energy we apply Lagrange's equation to obtain an expression for equations of the flexible body which is used in ADAMS.

$$M\ddot{\xi}+\dot{M}\dot{\xi}-\frac{1}{2}\left[\frac{\partial M}{\partial \xi}\dot{\xi}\right]\dot{\xi}+K\xi+f_g+D\dot{\xi}+\left[\frac{\partial \Psi}{\partial \xi}\right]^T\lambda=Q$$

Where K and D denote the stiffness and damping matrices for the flexible body.

The damping and stiffness effects are only deformation dependent and do not contribute to rigid body rotation and translation. Gravitational forces are written as f_g. Where λ denotes the Lagrange multipliers of the constraint equations ϕ, and Q the externally applied loads.

Application Example: Engine Accessory Belt Drive

The ADAMS belt-driven model consists of seven parts and the belt. These parts include the crank pulley, air conditioner pulley, the power-steering pump pulley, the water pump pulley, the alternator pulley, the automatic tensioner pulley, and the tensioner. The belt consists of 194 segments that are connected to each other with non-linear flexible elements. These components are configured with the belt in the manner shown in Figure 1 below.

$$\zeta=\begin{Bmatrix} x \\ y \\ z \\ \psi \\ \theta \\ \phi \\ q_l, j=1,m \end{Bmatrix}=\begin{Bmatrix} \mathbf{x} \\ \Psi \\ \mathbf{q} \end{Bmatrix}$$

The belt model is created using a discretized, lumped parameter analysis. Each part is represented by some geometry and a marker, with the material properties considered to be uniform throughout the part. The interaction between the parts is modeled using the FIELD statement in ADAMS.

The FIELD statement contains matrices for the viscous damping and stiffness between two adjacent elements, the preload force on the parts, the length between the two part markers, and an option to create a non-linear force function, which uses field subroutines. This function writes the FIESUB evaluation subroutine that calculates the six field components based on the components themselves and their derivative as a function of time and of the field I marker component displacements and component velocities with respect to the J marker. The FIESUB evaluation subroutine output must be strictly a function of the values in arrays DISP and VELO.

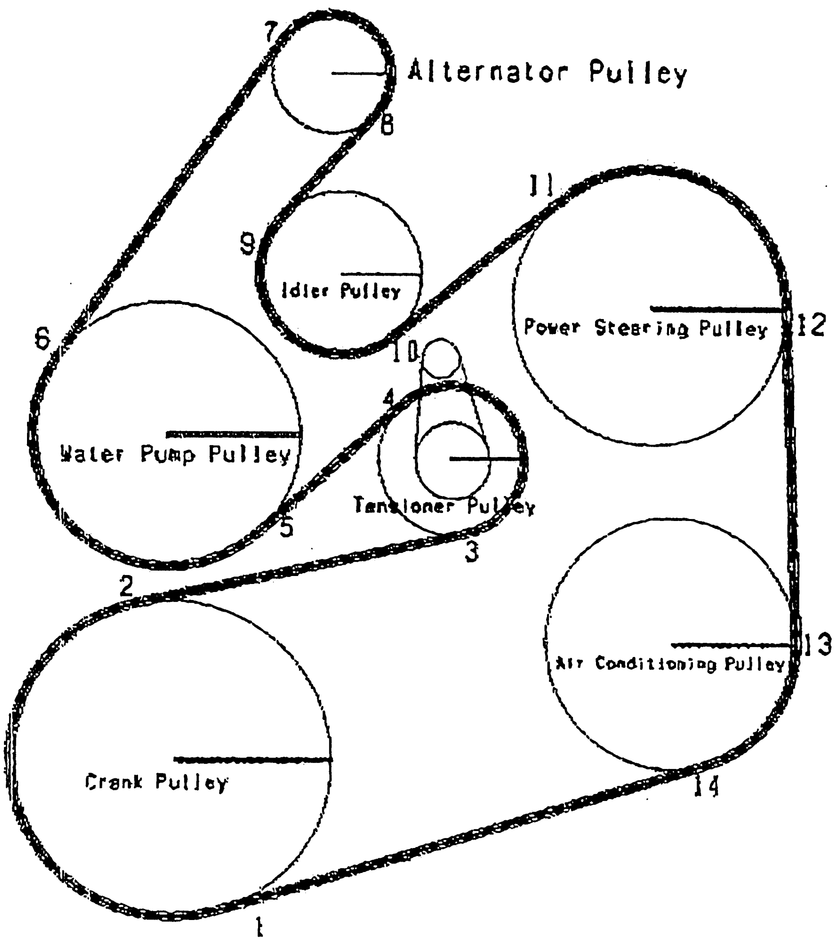

Figure 1. A typical engine accessory belt drive configuration

In this paper, the outline of the formulation of beam element stiffness matrices for the subroutines is presented as the method used in the model's calculations of stiffness. It is assumed that the parts can deform both axially and in bending. This is a superposition of a bar element (linear axial displacement) and a beam element (rotational bending). Since a lumped parameter analysis is assumed, the stiffness matrix for the constant stiffness is :

$$[\mathbf{k}] = \frac{AE}{L} = \begin{bmatrix} 1 & 0 & 0 & -1 & 0 & 0 \\ 0 & 0 & 0 & 0 & 0 & 0 \\ 0 & 0 & 0 & 0 & 0 & 0 \\ -1 & 0 & 0 & 1 & 0 & 0 \\ 0 & 0 & 0 & 0 & 0 & 0 \\ 0 & 0 & 0 & 0 & 0 & 0 \end{bmatrix} + \frac{EI}{L^3} \begin{bmatrix} 0 & 0 & 0 & 0 & 0 & 0 \\ 0 & 12 & 6L & 0 & -12 & 6L \\ 0 & 6L & 4L^2 & 0 & -6L & 2L^2 \\ 0 & 0 & 0 & 0 & 0 & 0 \\ 0 & -12 & -6L & 0 & 12 & -6L \\ 0 & 6L & 2L^2 & 0 & -6L & 4L^2 \end{bmatrix}$$

where: A = Cross-Sectional Area of the Beam
E = Modulus of Elasticity

I = Moment of Inertia
L = Length of the Beam

The stress stiffness matrices for beams is also determined, using an assumed lateral displacement field $w = w(x)$. An axial force, P, is presumed to be known in terms of the applied loads on the structure. Only in-plane displacements are considered, and the elements are placed on a local x-axis. Conventional strain terms, and a $w_{x}^{2}/2$ term to clearly show which terms lead to the conventional stiffness matrix and which to $[\mathbf{k}_{\sigma}]$.

The beam is assumed to have an axial displacement, $u = u(x)$ and a lateral displacement, $w = w(x)$. Membrane strain is $\varepsilon_m = u_{,x} + 0.5w_{,x}$. At a distance z from the centroid axis the axial strain contribution to the bending is $\varepsilon = -zw_{,xx}$, making the total axial strain at any location

$$\varepsilon_x = u_{,x} + 0.5w_{,x}^2 - zw_{,xx}$$

The stress is uniaxial at every point. This leads the strain energy of the element to be

$$U = \int_{V_e} \frac{1}{2} E\varepsilon_x^2 dV = \int_0^L \int_A \frac{1}{2} E\varepsilon_x^2 dA dx$$

Combining the above two equations, it can be found that

$$U = \int_0^L \frac{AE}{2} u_{,x}^2 dx + \int_0^L \frac{P}{2} w_{,x}^2 dx + \int_0^L \frac{EI}{2} w_{,xx}^2 dx \qquad [1]$$

Noting that

$$\int_A dA = A$$

$$\int_A z dA = 0$$

$$\int_A z^2 dA = I$$

$$\int_A E u_{,x} dA = P$$

The first integral of equation [1] yields the stiffness matrix for a bar element. The second integral contains the stress stiffness. The third integral yields the stiffness matrix for a standard beam element. For example, if the axial stiffness of the belt is 1200N per 1%. The stiffness per 10 mm (Assume the length of each chain segment is 10 mm) is

$$k_{11} = \frac{AE}{L} = \frac{1200}{0.01*10} = 12000\frac{N}{mm}$$

Let the bending stiffness be

$$EI = 4.8kg \cdot cm^2 = 4800N \cdot mm^2$$

This leads to the following

$$k_{55} = \frac{12EI}{L^3} = \frac{12*4800}{10^3} = 57.6\frac{N}{mm}$$

$$k_{56} = -\frac{6EI}{L^2} = -\frac{6*4800}{10^2} = -28.8N$$

$$k_{66} = \frac{4EI}{L} = \frac{4*4800}{10} = 1920N \cdot mm$$

Analysis

The following plots are from an analysis run of the belt-driven model. The engine speed for the analysis was 6000 rpm. The complete request file consists of 84 plots. This is a sample of the most interesting plots. The plots include belt tension, resultant forces acting on the crank, alternator power steering, water pump, air conditioning and tensioner.

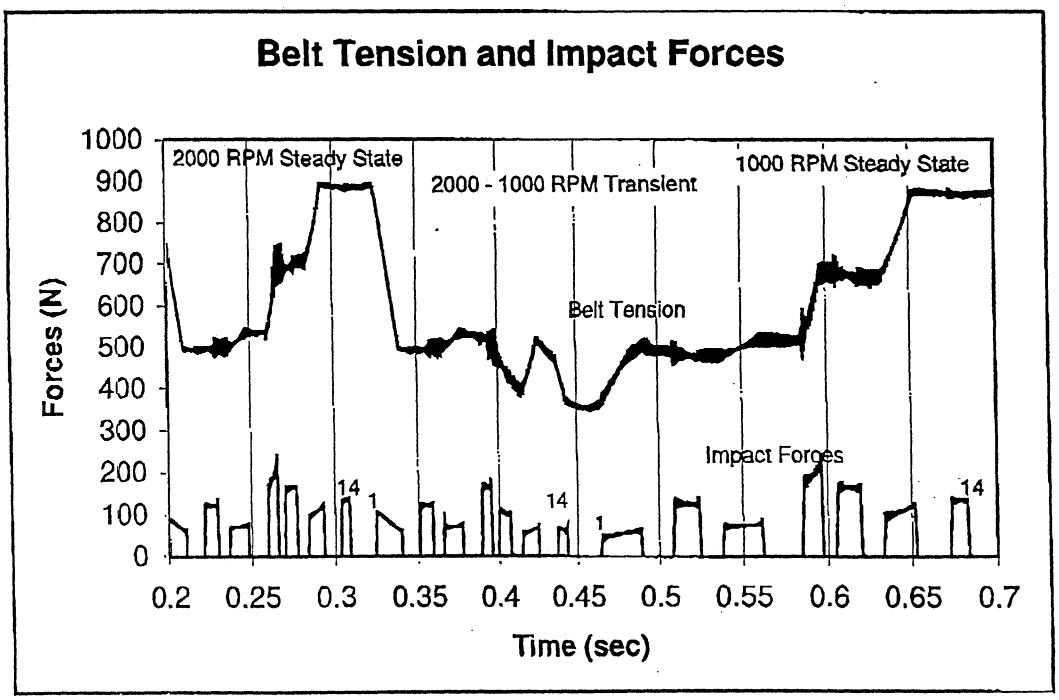

Figure 2. Belt tension and impact forces

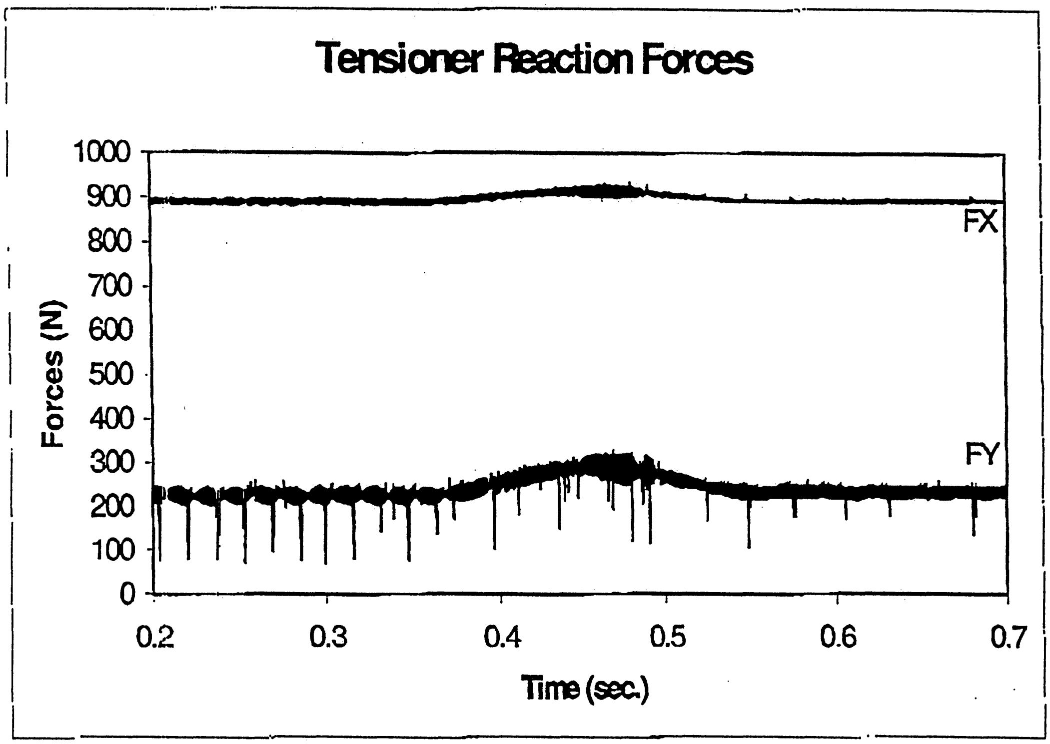

Figure 3. Reaction forces at the tensioner pulley

Figure 2 Shows the belt tension and impact forces between the pulleys and the belt. The simulation results can predict the vibration frequencies of each span as well as the tension in the belt between the pulleys. Between the simulation times of 200 milliseconds and 350 milliseconds, a 2000 RPM steady state behavior is prescribed. During the simulation times of 350 and 550 milliseconds there is a transient belt velocity from 2000 to 1000 RPM. The impact force changes do to the speed because of the transition of the belt from the tension side to the slack side of the pulley.

Figure 3 shows the reaction forces in the x and y directions on the tensioner pulley. Application of spectrum analysis can be used with this data to predict the nose level on the vibration modes. Using this information, engineers can investigate the belt behavior under different conditions of stiffness and friction in order to determine the optimal design. Also, the tension behavior during acceleration and deceleration conditions can be predicted.

Future work

Now that development and validation of the belt drive methodology has been completed, future work will continue in two areas. The current functionality will continue to be applied for various configurations in order to provide additional verification and experience in its application. In addition, development will proceed to provide additional functionality in the areas of noise calculation and in belt life cycle prediction.

The belt drive simulation functionality continues to be implemented in different applications in order to increase the bounds of its functionality and to provide engineers with expertise in applying the method. The preprocessor continues to be made more general as new configurations are required. The data from validation tests continue to provide information for the accuracy and sensitivity for various input and output parameters. During this time, the knowledge gained from "field testing" will be used to continuously verify and improve both the methodology and the application.

In order to make the tool more useful for engineers in related disciplines, additional functionality will be added as opportunities arise. There are currently two considerable development enhancements in the areas of noise calculation and life cycle prediction. These enhancements will materialize as a combination of enhanced internal functionality and added external communication support.

Noise prediction is an important issue in the analysis of belt drive mechanisms. Providing belt drive mechanisms with reduced noise profiles is critical for commercial products such as commercial automobiles. In addition, noise problems are usually an indicator of undesirable system modes, stresses, and forces. It is useful to investigate the noise characteristics in order to create an optimal design. The analysis of noise propagation is generally handled by software that is designed for that specific purpose. Current belt drive simulation development is focused on interfacing with such software in order to provide input to the noise prediction software.

Another important factor in the analysis of belt drive mechanisms is belt life cycle predictions. Life cycle prediction is used to determine whether a design meets acceptable criteria for the intended application. In the case of commercial automobiles, for example, long life cycles are required in order to meet warranty requirements. The calculations for life-cycle estimates are common and well known. Current work with the belt drive analysis software involves creating a method for automating these calculations based on the results of the dynamics analysis as post-processing step. This will provide engineers with immediate indications of whether or not a particular configuration will meet the life-cycle requirements.

These developments in the areas of noise calculation and life cycle prediction will continue until they reach a level of validation and expertise such that they are viable for general use. In addition, development in other areas will be evaluated and undertaken as the need arises in order to continue to provide a complete belt drive analysis capability.